Darcy–Carreau–Yasuda rheological model and onset of inelastic non-Newtonian mixed convection in porous media

Darcy-Carreau-Yasuda rheological model and onset of inelastic non-Newtonian mixed convection in porous media

P.V. Brandão.,[1, a)] M.N. Ouarzazi,[2, b)] S. Hirata,[2, c)] and A. Barletta[1, d)]
[1)] *Department of Industrial Engineering, Alma Mater Studiorum Università di Bologna, Viale Risorgimento 2, Bologna 40136, Italy.*
[2)] *Unité de Mécanique de Lille, Joseph Boussinesq, EA 7512, Université de Lille, Bd. Paul Langevin, 59655 Villeneuve d'Ascq Cedex, France.*

(Dated: 28 March 2021)

An extension of Carreau and Carreau-Yasuda rheological models to porous media is proposed to study the onset of mixed convection of both pseudoplastic fluids (PF) and dilatant fluids (DF) in a porous layer heated from below in the presence of a horizontal throughflow. In comparison to Newtonian fluids, three more dimensionless parameters are introduced, namely the Darcy-Weissenberg number Wi, the power-law index n and the Yasuda parameter a. Temporal stability analysis of the basic state showed that in the absence of a throughflow ($Wi = 0$), the critical Rayleigh number and the critical wavenumber at the onset of convection are the same as for Newtonian fluids, namely $Ra_c = 4\pi^2$ and $k_c = \pi$ respectively. When the throughflow is added ($Wi > 0$), it is found that moving transverse rolls (stationary longitudinal rolls) are the dominant mode of the instability for PF (for DF). Furthemore, depending on Wi, two regimes of instability were identified. In the weakly non-Newtonian regime (i.e. $Wi < Wi_t \approx 1$) a destabilising effect is observed for PF while the reverse occurs for DF. These effects are more intense by reducing (increasing) the index n for PF (for DF). In this regime, a significant qualitative difference is found between the Darcy-Carreau model and the power-law model. However in the strongly non-Newtonian regime, the two models lead to similar results. A mechanical energy budget analysis is performed to understand the physical effects of the interaction between the basic throughflow and the disturbances. It is also shown that the intrinsic macroscale properties of the porous medium may play a key role in the stabilizing/destabilizing effect. Finally, a comparison is made between the present theoretical predictions and recent mixed convection experiments in a Hele-Shaw cell.

I. INTRODUCTION

In the last decades, a considerable amount of work has been done to assess the physical characteristics of the Rayleigh-Bénard instability in fluid saturated porous media. There are several surveys on this subject available in the literature. We mention Chapter 4 of the book by Straughan[1], Chapter 6 of the book by Nield and Bejan[2], as well as Chapter 7 of the book by Barletta[3]. As is well-known, the driving mechanism of the Rayleigh-Bénard instability is the upward temperature gradient imposed across the fluid saturated medium via the thermal conditions at the plane horizontal boundaries of the layer. In the classical setup, such conditions entail different uniform temperatures at the two bounding planes. Most studies on the Rayleigh-Bénard instability in porous media involve a Newtonian fluid whose momentum transfer is modelled by Darcy's law. However, there has been a significant and growing interest for the case where the saturating fluid is non-Newtonian. Either viscous or viscoelastic rheology has been envisaged[4–9]. The interest for non-Newtonian fluids is mainly due to the many applications related to geophysics or fuel engineering, where the underground fluids seeping through rocks or sand, in several cases, do not follow the simple Newtonian rheology. For the special case of viscous fluids, the simplest non-Newtonian model is power-law. We mention that the extension of Darcy's law to power-law fluids was formulated in the pioneering work by Christopher and Middleman[10]. This model has been employed by Barletta and Nield[4] in a study of the Rayleigh-Bénard instability of both pseudoplastic and dilatant fluids in a porous layer heated from below in the presence of horizontal throughflow. The preferred mode of instability was found to be transverse rolls for pseudoplastic fluids and longitudinal rolls for dilatant fluids. In the limit of the Darcy-Bénard problem without throughflow, the linear stability results showed that the critical Rayleigh number tends to infinity for shear-thinning fluids and tends to zero for shear-thickening fluids[4]. These last results are simply a consequence of the main drawback of the power-law model with its intrinsic singularity when the shear rate tends to zero or, in the case of porous media, when the seepage velocity tends to zero. We mention that the limits of power–law model to analyse Darcy-Bénard convection were pointed out by Nield[11,12]. To overcome these limits, Brandão and Ouarzazi proposed in a recent paper[13] a novel Darcy-Carreau rheological model for the viscosity of non-Newtonian inelastic fluids flowing through a porous medium. In the paper by Brandão and Ouarzazi[13], both linear and weakly nonlinear stability analyses were performed for Darcy-Bénard convection of pseudoplastic fluids and dilatant fluids. It is found that that the critical Rayleigh number and wave number corresponding to the onset of convection are the same as for Newtonian fluids. The influence of rheological parameters on the nature of the bifurcation is discussed by using weakly nonlinear theory. It is found that the bifurcation from the conduction state to convection rolls is always supercritical for dilatant fluids. For pseudoplastic fluids, however, shear-thinning

[a)] Electronic mail: pedro.vayssiere2@unibo.it
[b)] Electronic mail: mohamed-najib.ouarzazi@univ-lille.fr
[c)] Electronic mail: silvia.hirata@univ-lille.fr
[d)] Electronic mail: antonio.barletta@unibo.it

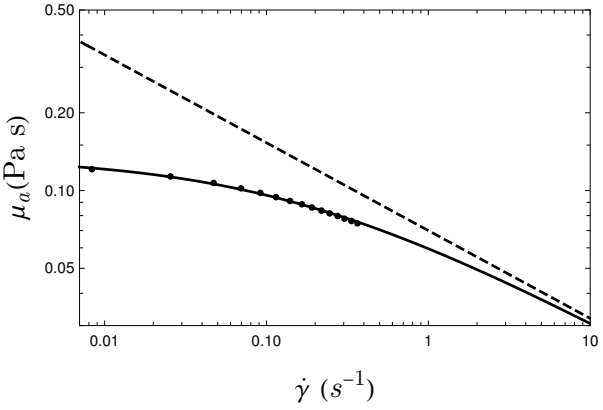

FIG. 1. Measured data (points) in experiment 4 extracted from[15] and its supplementary material and fitted Carreau-Yasuda rheological model (continuous line). The dashed line corresponds to the power–lawer predictions.

character of these fluids may induce a subcritical bifurcation. We mention that, in a recent paper[14], Rees showed that convection of Bingham fluids saturating a porous medium also appears via a subcritical bifurcation.

From the experimental viewpoint, Petrolo et al.[15], conducted a set of experiments in a Hele-Shaw cell to study the flow patterns in Rayleigh-Bénard instability of pseudoplastic fluids in the presence of horizontal throughflow. The experiments were carried out with Xanthan Gum mixtures with different concentrations as working fluids. In addition, a two-dimensional linear stability analysis is proposed in that paper. The fluid is taken to be of power law nature with temperature dependent consistency index. Comparison between linear stability analysis and experiments pointed out: i) a good agreement between theory and experiments concerning the critical wave number of the instability. ii) the disagreement between experiments and theory is significant for the critical Rayleigh number, but the trend is correctly reproduced in particular for the high Péclet number experiments, with the theory overestimating the experiments by a maximum factor less than two.

The objective of the present work is to revisit the Rayleigh-Bénard convection problem in the presence of a uniform cross-flow in porous media as well as in Hele-Shaw cells. The non-Newtonian fluid rheological behavior is described by employing the Carreau-Yasuda model[16] extended to porous media. The next section gives more details about this model. It has the advantage to be a regular model which combines the power-law region for sufficiently high shear rate and the Newtonian region of the viscosity curve for weak shear rate. It also contains five parameters to interpret the rheology of the fluid and to fit experimental viscosity curves (see section IV B). Figure 1 shows the viscosity distribution as a function of the shear rate predicted by both the Carreau-Yasuda and the power-law models with measured viscosity data[15]. It can be seen from this figure that the power law model overestimates the apparent viscosity in the region of small shear-rate where the thermal instability was observed experimentally.

A. Darcy-Carreau-Yasuda rheological model

In a fluid medium without a solid matrix, the simplest rheological model usually employed to describe the behaviour of non-Newtonian visco-inelastic fluid is the power-law model given by

$$\tau = \eta\, \dot{\gamma}^n \tag{1}$$

in which τ [Pa], $\dot{\gamma}$ [s^{-1}], η [Pas^n] and n are the shear stress, the shear rate, the consistency factor and the power-law exponent, respectively. The fluid acts like shear thinning (pseudoplastic fluid) and shear thickening (dilatant fluid) for $n < 1$ and $n > 1$, respectively, while $n = 1$ means Newtonian fluid. In the latter case, η is the Newtonian viscosity μ_0.

The expression of the apparent viscosity defined as $\mu_a = \frac{\tau}{\dot{\gamma}}$ is,

$$\mu_a = \eta\, \dot{\gamma}^{n-1} \tag{2}$$

For porous media, after integration over a representative elementary volume, the power–law model introduces the following apparent viscosity,

$$\mu_a = \eta_{ef}\, |\mathbf{V}^*|^{n-1} \tag{3}$$

where η_{ef} [Pas^n m^{1-n}] is the effective consistency factor and $\mathbf{V}^*$ is the filtration velocity.

From expressions (2) and (3) of the apparent viscosity μ_a, we define a porous shear stress $\dot{\gamma}_p^*$ as

$$\dot{\gamma}_p^* = \left(\frac{\eta_{ef}}{\eta}\right)^{\frac{1}{n-1}} |\mathbf{V}^*| \tag{4}$$

The ratio $\frac{\eta_{ef}}{\eta}$ depends in general on the permeability K, the power–law exponent n and the porosity Φ of the porous medium. An expression of this ratio was used by many authors as, for example, Pascal et al.[18] and Longo et al.[19]. It reads,

$$\frac{\eta_{ef}}{\eta} = f_p\, (\Phi K)^{\frac{1-n}{2}} \tag{5}$$

with $f_p = 8^{(-\frac{n+1}{2})}\, 2\, (\frac{3n+1}{n})^n$.

Therefore the porous shear rate (4) may be written as

$$\dot{\gamma}_p^* = f_p^{\frac{1}{n-1}}\, (\Phi K)^{-1/2}\, |\mathbf{V}^*| \tag{6}$$

Considering the shear thinning fluid ($n < 1$), one of the problems dealing with the power–law model is that it gives infinite apparent viscosity for a vanishing shear stress in a fluid clear of solid material and for a zero velocity in a porous medium. In these limits, the power–law model predicts zero viscosity for a shear thickening fluid ($n > 1$).

To overcome these singularities in a fluid medium, a regularized form of the power–law model is used, namely the Carreau-Yasuda model given by

$$\frac{\mu - \mu_\infty}{\mu_0 - \mu_\infty} = (1 + (\lambda^* \dot{\gamma})^a)^{\frac{n-1}{a}} \tag{7}$$

The positive constant a is the Yasuda parameter that represents the transition region between the zero shear rate region and the power-law region. Incidentally, we stress that the rheological model adopted in this paper does not include the effect of temperature variation of the apparent viscosity taken into account in the paper by Petrolo et al.[15]. When $a=2$, the Carreau model is recovered. The constant μ_∞ is the infinite shear rate viscosity and λ^* is a characteristic time of the non-Newtonian fluid defined as,

$$\lambda^* = (\frac{\eta}{\mu_0})^{\frac{1}{n-1}} \tag{8}$$

Usually, μ_∞ is negligible[17] and then the Carreau-Yasuda model reads

$$\frac{\mu}{\mu_0} = (1+(\lambda^*\dot{\gamma})^a)^{\frac{n-1}{a}} \tag{9}$$

In the same way, the singularities of the power–law model applied to a porous medium, may be avoided in the limit of zero filtration velocity $\mathbf{V}^*$ by adopting the following proposed rheological model:

$$\frac{\mu_a}{\mu_0} = \left(1+\left(\frac{\eta_{ef}}{\mu_0}\right)^{\frac{a}{n-1}}|\mathbf{V}^*|^a\right)^{\frac{n-1}{a}} \tag{10}$$

We note that, in the limit of large $|\mathbf{V}^*|$, the power–law model (3) is recovered, while the viscosity takes a finite non-zero value $\mu=\mu_0$ in the limit of a vanishing $|\mathbf{V}^*|$, independently of n. In this limit, the fluid behaviour is Newtonian.

By introducing the characteristic time of the fluid λ^* defined by (8) and the ratio $\frac{\eta_{ef}}{\eta}$ defined by (5) for porous media, equation (10) may be written as a Darcy-Carreau-Yasuda model similar to (9),

$$\frac{\mu_a}{\mu_0} = \left(1+(\lambda^*\dot{\gamma}_p^*)^a\right)^{\frac{n-1}{a}} \tag{11}$$

For practical reasons, the governing equations of the problem for the non-Newtonian fluid will be formulated based on the generalized Darcy-Carreau-Yasuda model (11), where we introduce the explicit expression (6). In that case, the generalized Darcy-Carreau-Yasuda model (11) yields,

$$\frac{\mu_a}{\mu_0} = \left(1+(\lambda^* f_p^{\frac{1}{n-1}}(\Phi K)^{-1/2}|\mathbf{V}^*|)^a\right)^{\frac{n-1}{a}} \tag{12}$$

B. Governing equations

Let us consider an isotropic and homogeneous plane porous channel of height H and of infinite extension in the horizontal plane where a shear-thinning fluid or shear-thickening fluid is flowing at a constant velocity U_0^* in the x direction. The system is heated from below and cooled from above. The upper and lower horizontal walls are considered impermeable and are kept at constant temperatures T_1^* and T_0^*, respectively. We assume that the Oberbeck-Boussinesq approximation holds. The rheological model used for the apparent viscosity is supposed to comply with the Darcy-Carreau-Yasuda model (12). The continuity, momentum and energy equations, as well as the Darcy-Carreau-Yasuda rheological model, can then be written as

$$\nabla\cdot\mathbf{V}^* = 0 \tag{13}$$

$$\frac{\mu_a}{K}\mathbf{V}^* + \nabla P^* - \rho_0\beta(T^*-T_1^*)\mathbf{g} = 0 \tag{14}$$

$$(\rho c)_m\frac{\partial T^*}{\partial t^*} + (\rho c)_f\mathbf{V}^*\cdot\nabla T^* = k_m\nabla^2 T^* \tag{15}$$

$$\frac{\mu_a}{\mu_0} = \left(1+(\lambda^* f_p^{\frac{1}{n-1}}(\Phi K)^{-1/2}|\mathbf{V}^*|)^a\right)^{\frac{n-1}{a}} \tag{16}$$

The boundary conditions at the impermeable and perfectly conducting horizontal walls are:

$$\begin{aligned} &T^* = T_0^* \ \text{ at } \ z^*=0 \ \text{ and } \ T^* = T_1^* \ \text{ at } \ z^*=H \\ &W^* = 0 \ \text{ at } \ z^*=0,H \end{aligned} \tag{17}$$

where $(U^*,V^*,W^*)=\mathbf{V}^*$ denote the Cartesian components of the velocity field, T^* is the temperature field, P^* is the hydrostatic pressure field, μ_a is the apparent dynamic viscosity, μ_0 is the dynamic viscosity at the zero shear rate, k_m is the effective thermal conductivity, β is the fluid thermal expansion coefficient, K is the permeability, ρ is the fluid density, $(\rho c)_m$ and $(\rho c)_f$ are the heat capacity per unit volume of the saturated porous medium and the heat capacity per unit volume of the fluid, respectively. Finally, $\mathbf{g}=-g\mathbf{e_z}$ is the gravitational acceleration, with g denoting its modulus and $\mathbf{e_z}$ the unit vector along the z axis.

According to the energy equation (15) and the boundary conditions (17), the basic solution for the temperature corresponds to a vertical thermal stratification:

$$T_{(b)}^* - T_1^* = (1-z^*/H)(T_0^*-T_1^*) \tag{18}$$

A horizontal throughflow is imposed,

$$\mathbf{V}^*_{(b)} = U_0^*\,\mathbf{e_x} \tag{19}$$

which generates, according to (16), a variation of the basic apparent viscosity,

$$\frac{\mu_{a(b)}}{\mu_0} = \left(1+\left(\lambda^* f_p^{\frac{1}{n-1}}(\Phi K)^{-1/2}U_0^*\right)^a\right)^{\frac{n-1}{a}} \tag{20}$$

According to the definition (6), the term $f_p^{\frac{1}{n-1}}(\Phi K)^{-1/2}U_0^*$ represents the basic porous shear rate $\dot{\gamma}_{p(b)}$. Consequently, the term $\lambda^* f_p^{\frac{1}{n-1}}(\Phi K)^{-1/2}U_0^*$ is the product of the basic porous shear rate $\dot{\gamma}_{p(b)}$ and the characteristic time λ^* of the fluid. This product is known in the literature about non-Newtonian fluids flowing in a cavity without a solid matrix as Weissenberg

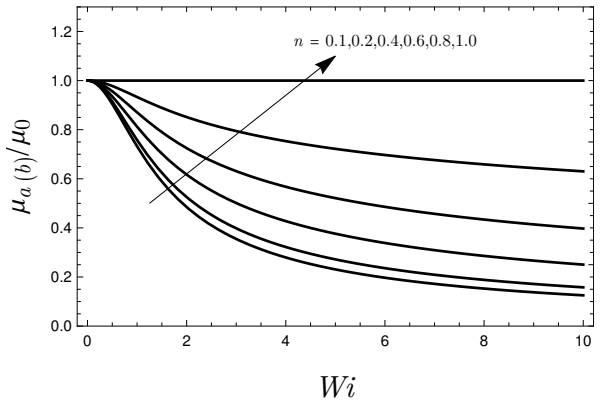

FIG. 2. Apparent viscosity normalised by the viscosity at zero shear rate μ_0 versus Darcy-Weissenberg number for $a = 2$ and different values of n: pseudoplastic fluids.

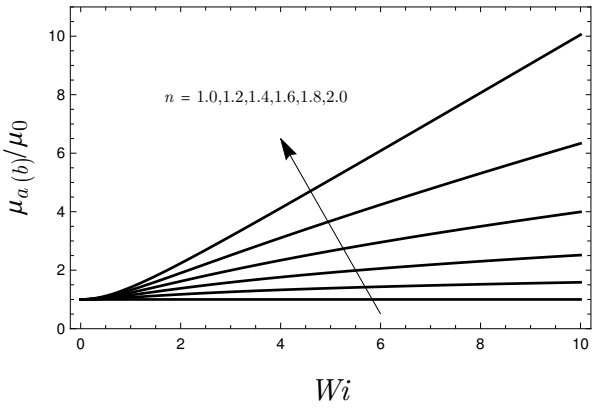

FIG. 3. Apparent viscosity normalised by the viscosity at zero shear rate μ_0 versus Darcy-Weissenberg number for $a = 2$ and different values of n: dilatant fluids

number. As we are dealing with porous media, we define the Darcy-Weissenberg number as,

$$Wi = \lambda^* \dot{\gamma}^*_{p(b)} \tag{21}$$

which may be seen as a measure of the influence of non-Newtonian forces on the flow saturated a porous medium. By introducing this number, equation (20) takes the form,

$$\frac{\mu_{a(b)}}{\mu_0} = (1 + Wi^a)^{\frac{n-1}{a}} \tag{22}$$

The influence of the non-Newtonian nature of the fluid on the apparent viscosity depends on the three dimensionless numbers: Wi, n and a.

The special case of $n = 1$ or $\lambda^* = 0$ and then $Wi = 0$ represents a Newtonian fluid with viscosity μ_0, independently of U_0^*. As proved by Prats[24], in this case, the onset of convection happens with critical wavenumber and Rayleigh number independent of the throughflow velocity U_0^*.

It is also important to consider the interesting limit of a zero throughflow, $U_0^* = 0$, for a non-Newtonian fluid with $n \neq 1$ and $\lambda^* \neq 0$. In this limit, the Darcy-Weissenberg number is zero, and according to (22), the viscosity is constant and equal to the viscosity μ_0 of the non-Newtonian fluid in the limit of zero porous shear rate. Therefore, we can expect that, in the case of $U_0^* = 0$, the convection for a non-Newtonian fluid may arise under the same conditions as for a Newtonian fluid.

For the general case, Figs. 2 and 3 show the variation of $\frac{\mu_{a(b)}}{\mu_0}$ as a function of Wi for $a = 2$ (i.e. Darcy-Carreau model) and for different values of n for pseudoplastic and dilatant fluids, respectively. Figure 2 states that the effect of increasing Darcy-Weissenberg number for a fixed value of n is to decrease the apparent viscosity, making then the fluid more shear thinning, for the pseudoplastic case. The decrease of the apparent viscosity is more effective when n decreases, thus further enhancing the shear thinning characteristic of the fluid. The contrary effect is observed for dilatant fluids.

We note that the influence of the Yasuda parameter a on the apparent viscosity may be significant in two regions of the $(Wi, \frac{\mu_{a(b)}}{\mu_0})$ plane, namely a region where $Wi \to 0$ on one hand and a region where $Wi = O(1)$ on the other hand. When $Wi \gg 1$, Eq. (22) yields,

$$\frac{\mu_{a(b)}}{\mu_0} = Wi^{n-1} \tag{23}$$

In this limit, the apparent viscosity is then given by the power-law rheological model and it does not depend on the parameter a.

From Eq.(14), we note that the horizontal basic pressure gradient is influenced by the non-Newtonian nature of the fluid,

$$-\frac{\partial P^*_{(b)}}{\partial x^*} = \frac{\mu_0}{K}(1 + Wi^a)^{\frac{n-1}{a}} U_0^* \tag{24}$$

Furthermore, the buoyancy force generates a vertical pressure gradient,

$$\frac{\partial P^*_{(b)}}{\partial z^*} = -\rho_0 \beta (1 - z^*/H)(T_0^* - T_1^*) \tag{25}$$

II. DIMENSIONLESS EQUATIONS AND LINEAR STABILITY ANALYSIS

A. Dimensionless equations

We choose $H, k_m/(H(\rho c)_f), H^2(\rho c)_m/k_m, k_m\mu_0/(K(\rho c)_f)$ and $\Delta T^* = T_0^* - T_1^*$, as reference quantities for length, velocity, time, pressure and temperature $(T^* - T_1^*)$. With this scaling, the following set of dimensionless equations is obtained:

$$\nabla \cdot \mathbf{V} = 0 \tag{26}$$

$$(1 + (\alpha |\mathbf{V}|)^a)^{\frac{n-1}{a}} \mathbf{V} + \nabla P - Ra T \mathbf{e_z} = 0 \tag{27}$$

$$\frac{\partial T}{\partial t} + \mathbf{V}\cdot\nabla T - \nabla^2 T = 0 \tag{28}$$

with $\alpha = \lambda^* f_p^{\frac{1}{n-1}} (\Phi K)^{\frac{-1}{2}} \kappa_m / H$, where $\kappa_m = k_m/(\rho c)_f$ is the thermal diffusivity of the porous medium. It may be written for a non-zero Pe as

$$\alpha = \frac{Wi}{Pe} \tag{29}$$

The dimensionless boundary conditions are

$$\begin{aligned} &T = 1 \quad \text{at} \quad z = 0 \quad \text{and} \quad T = 0 \quad \text{at} \quad z = 1 \\ &W = 0 \quad \text{at} \quad z = 0, 1 \end{aligned} \tag{30}$$

The basic state may be written in dimensionless form as,

$$T_{(b)} = 1 - z \tag{31}$$

$$\mathbf{V}_{(b)} = Pe\,\mathbf{e_x} \tag{32}$$

$$\nabla P_{(b)} = -(1+Wi^a)^{\frac{n-1}{a}}\, Pe\,\mathbf{e_x} + Ra\,T_{(b)}\,\mathbf{e_z} \tag{33}$$

In addition to the Darcy-Weissenberg number, the power-law exponent n and the Yasuda parameter a, two further dimensionless parameters are introduced:

- the filtration Rayleigh number

$$Ra = \frac{\rho_0 K H g \beta \Delta T^*}{\kappa_m \mu_0} \tag{34}$$

- the Péclet number

$$Pe = \frac{U_0^* H (\rho c)_f}{\kappa_m} \tag{35}$$

B. Linear stability formulation

To investigate the stability of the conductive state, infinitesimal three-dimensional perturbations are superposed to the basic solution,

$$\mathbf{V} = Pe\,\mathbf{e_x} + \mathbf{v}(x,y,z,t),$$

$$T = T_{(b)} + \theta(x,y,z,t),\;\; P = P_{(b)} + p(x,y,z,t) \tag{36}$$

Substituting equations (36) into (26)-(28), we obtain after linearizing the system,

$$(1+Wi^a)^{\frac{n-1}{a}} \left[\mathbf{v} + \frac{(n-1)Wi^a}{1+Wi^a}\,\mathbf{v}.\mathbf{e_x}\right] = -\nabla p + Ra\,\theta\,\mathbf{e_z} \tag{37}$$

$$\frac{\partial \theta}{\partial t} + Pe\frac{\partial \theta}{\partial x} - w - \nabla^2\theta = 0, \tag{38}$$

Taking the double curl of the momentum equation (37) and by using continuity equation, one obtains a set of two coupled equations involving the vertical component of the velocity perturbation w and the temperature perturbation θ, namely

$$(1+Wi^a)^{\frac{n-1}{a}} \left[\nabla^2 - \frac{(n-1)Wi^a}{1+nWi^a}\frac{\partial^2}{\partial x^2}\right] w - Ra\left[\nabla_2^2 - \frac{(n-1)Wi^a}{1+nWi^a}\frac{\partial^2}{\partial x^2}\right]\theta = 0, \tag{39a}$$

$$\frac{\partial \theta}{\partial t} + Pe\frac{\partial \theta}{\partial x} - w - \nabla^2\theta = 0, \tag{39b}$$

where ∇_2^2 is the two-dimensional Laplacian in the (x,y) plane. These equations are subject to the boundary conditions

$$w = \theta = 0, \quad \text{at} \quad z = 0 \quad \text{and} \quad z = 1. \tag{40}$$

C. Dominant mode of instability

The three-dimensional disturbance quantities $w(x,y,z,t)$ and $\theta(x,y,z,t)$ satisfying the boundary conditions (30) are expressed as

$$[w,\theta] = \left[\tilde{w},\tilde{\theta}\right] \exp(ik_x x + ik_y y - i\,\omega t)\sin(\pi z) \tag{41}$$

where k_x and k_y are the wavenumbers in the x and y direction, respectively, and ω is the complex frequency. Its imaginary part $Im(\omega)$ and real part $Re(\omega)$ represent, respectively, the temporal growth rate and the frequency of the unstable perturbations.

The neutral temporal stability condition is obtained by imposing $Im(\omega) = 0$, which selects dominant modes at the onset of convection. By substituting equations (41) into (39), we obtain the dispersion relation

$$\mathscr{D}\left(k_x, k^2, Ra, Re(\omega), Wi, n, a\right) = 0, \tag{42}$$

where $k^2 = k_x^2 + k_y^2$. The imaginary part of this relation gives: $Re(\omega) = k_x Pe$. By substituting this result into the real part of the relation, we get

$$\left(k^2+\pi^2\right)(1+Wi^a)^{\frac{n-1}{a}} \left[-\left(k^2+\pi^2\right) + \frac{(n-1)Wi^a}{1+nWi^a}k_x^2\right] - Ra\left[-k^2 + \frac{(n-1)Wi^a}{1+nWi^a}k_x^2\right] = 0 \tag{43}$$

From (43) it is possible to recover an explicit equation for Ra from the neutral stability condition, namely

$$Ra = (k^2+\pi^2)(1+Wi^a)^{\frac{n-1}{a}} \times \left(1 + \frac{\pi^2(1+nWi^a)}{k^2(1+nWi^a) - (n-1)k_x^2 Wi^a}\right) \tag{44}$$

Equation (44) can be equivalently written in a more generic way, by adopting the relation $k_x = k\cos(\phi)$. In that case, $\phi = 0$

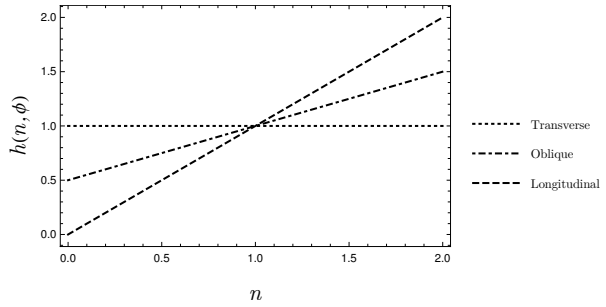

FIG. 4. Function $h(n,\phi)$ versus n for convective rolls with different values of the inclination angle ϕ

.

represents the case of tranverse rolls, $\phi = \pi/2$ the longitudinal rolls and $0 < \phi < \pi/2$ the oblique rolls. For each parametric combination, (Wi,n,a), the neutral value of Ra is recovered for each value of k and ϕ. In order to have the critical condition one can take the derivative of (44) with respect to k, assuming $k_x = k\cos(\phi)$, and evaluate the zeros of the resulting expression. It yields

$$k_c = \pi \left[\frac{1 + nWi^a}{1 + Wi^a\,(n + (1-n)\cos^2(\phi))} \right]^{\frac{1}{4}}, \qquad (45)$$

which, when substituted in (44), yields

$$Ra_c = \pi^2 \left(1 + Wi^a\right)^{\frac{n-1}{a}} \times \left[1 + \left(\frac{1 + nWi^a}{1 + Wi^a\,(n + (1-n)\cos^2(\phi))} \right)^{\frac{1}{2}} \right]^2. \qquad (46)$$

One can observe that, for a given parametric combination, the critical Ra depends also on the kind of rolls considered. It is interesting now to discuss the linear pattern selection, that is which kind of rolls will present the lowest value of Ra_c. On account of equation (46), one may realize that the dependence of the angle ϕ appears just in one term, and its role will depend also on the value of n. One may rewrite equation (46) as

$$Ra_c = \pi^2 \left(1 + Wi^a\right)^{\frac{n-1}{a}} \left[1 + \left(\frac{1 + nWi^a}{1 + Wi^a\,h(n,\phi)} \right)^{\frac{1}{2}} \right]^2, \qquad (47)$$

where

$$h(n,\phi) = n + (1-n)\cos^2(\phi), \qquad (48)$$

and conclusions regarding the pattern selection can be drawn by employing this quantity. If $n = 1$, the results are independent of ϕ and $h(n,\phi) = 1$. For $n \neq 1$, the lower values of Ra_c could depend on the higher values of $h(n,\phi)$. Since this function appears in the denominator, its maximum represents the minimum of Ra_c.

Figure 4 shows the dependence of the function $h(n,\phi)$ on n, considering three values of ϕ: $\phi = 0$ (transverse rolls), $\phi = \pi/4$ (oblique rolls) and $\phi = \pi/2$ (longitudinal rolls). It can be concluded from the figure that transverse rolls are the most unstable patterns for $n < 1$, while for $n > 1$ longitudinal rolls become the critical ones. Oblique rolls, represented here by $\phi = \pi/4$, are always in between.

The expressions of the critical values of Ra and k can be simplified for the transverse and the longitudinal cases, respectively, to

$$Ra_c^T = \pi^2 \left(1 + Wi^a\right)^{\frac{n-1}{a}} \left[1 + \left(\frac{1 + nWi^a}{1 + Wi^a} \right)^{\frac{1}{2}} \right]^2, \qquad (49a)$$

$$k_c^T = \pi \left[\frac{1 + nWi^a}{1 + Wi^a} \right]^{\frac{1}{4}}, \qquad (49b)$$

and

$$Ra_c^L = 4\pi^2 \left(1 + Wi^a\right)^{\frac{n-1}{a}}. \qquad (50a)$$

$$k_c^L = \pi. \qquad (50b)$$

It is very instructive to inspect the behaviour of Ra_c^T, Ra_c^L, and k_c^T in the limit of a very large Darcy-Weissenberg number ($Wi \gg 1$). Eqs. (49a), (49b) and (50a) yield in the asymptotic limit of a very large Wi,

$$Ra_c^T = \pi^2 \left(1 + n^{\frac{1}{2}}\right)^2 (Wi)^{n-1}, \qquad (51a)$$

$$k_c^T = \pi n^{\frac{1}{4}}, \qquad (51b)$$

$$Ra_c^L = 4\pi^2 (Wi)^{n-1}. \qquad (51c)$$

If we replace Wi in Eqs. (51a) and (51c) by its expression,

$$Wi = \lambda^* f_p^{\frac{1}{n-1}} (\Phi K)^{\frac{-1}{2}} U_0^* = \left(\frac{\eta_{ef}}{\mu_0} \right)^{\frac{1}{n-1}} \frac{\kappa_m}{H} Pe \qquad (52)$$

and defining a power–law Rayleigh number Ra^{pl}, commonly employed by many authors (see for example Barletta and Nield[4] and Petrolo et al.[15]),

$$Ra^{pl} = \frac{\rho_0 \beta\, g\, K\, H^n\, \Delta T^*}{\eta\, \kappa_m^n} \qquad (53)$$

where K represents a generalized permeability (SI units m^{n+1}), then Eqs. (51a) and (51c) yield,

$$Ra_c^{plT} = \pi^2 \left(1 + n^{\frac{1}{2}}\right)^2 (Pe)^{n-1}, \qquad (54a)$$

$$Ra_c^{plL} = 4\pi^2 (Pe)^{n-1}. \qquad (54b)$$

The above critical power–law Rayleigh numbers and the corresponding critical wavenumbers (51b) and (50b) are exactly the same as those derived in Barletta and Nield[4]. Consequently, this result shows that the theoretical predictions stemming from the power–law rhelogical model are recovered by using the Darcy-Carreau-Yasuda model in the limit of infinite Darcy-Weissenberg number. In this limit, the instabilty regime will be termed as strongly non-Newtonian.
For a small Darcy-Weissenberg number, a regime that we identify as weakly non-Newtonian, a Taylor expansion of Ra_c^T, Ra_c^L given respectively by Eqs. (49a), and (50a) yields

$$Ra_c^T = 4\pi^2 \left(1 + (n-1)(\frac{1}{2} + \frac{1}{a})Wi^a\right), \qquad (55a)$$

$$Ra_c^L = 4\pi^2 \left(1 + \frac{n-1}{a} Wi^a\right). \qquad (55b)$$

We note that, for $Wi = 0$, we recover the classical critical values $Ra_c = 4\pi^2$ and $k_c = \pi$ associated with the Horton-Rogers-Lapwood problem. This means that, in the absence of a throughflow and according to the present linear stability analysis, convection for a non–Newtonian fluid emerges under the same conditions as for a Newtonian one. In the Rayleigh-Bénard problem without a porous matrix, among the very few investigations on the thermal instability for shear thinning fluids, Darbouli et al.[20] conducted experiments with Xanthan–gum solutions at different concentrations. These experiments concluded that the onset of convection is observed for all the concentrations used around the Rayleigh value $Ra_c = 1800$ which corresponds to the Newtonian value. As thermal instability in porous media and in a fluid clear of solid material are qualitatively similar in a number of aspects, it is not a surprising prediction that the onset of convection in porous media corresponds to $Ra_c = 4\pi^2$, independently of the Newtonian or non-Newtonian nature of the fluid. We note that this result differs from the one derived in Barletta and Nield[4] in the limit of zero Péclet number, namely Ra_c^{plT} tends to infinity for shear thinning fluids and Ra_c^{plL} tends to zero for shear thickening fluids. These results were obtained in the framework of the power–law model which presents a singularity as *Pe* becomes small as it is pointed out in Section I A.

For the general case, the dependence on Wi of the critical Rayleigh number and the critical wave number at the onset of convection is presented for different values of n associated with pseudoplastic fluids ($n < 1$) and dilatant fluids ($n > 1$) and for different values of the Yasuda parameter a. Variations with Darcy-Weissenberg number of the critical Rayleigh number at the onset of transverse rolls for Newtonian ($n = 1$) and pseudoplastic ($n < 1$) fluids, with different values of n and $a = 2$, are depicted by solid lines in Fig. 5. Critical Rayleigh number is presented normalized by the classical value for Newtonian fluids $Ra_c = 4\pi^2$ in such a way that the detachment from Newtonian results can be observed clearly when Wi increases. Fig. 5 shows that with increasing Wi, $\frac{Ra_c^T}{4\pi^2}$ decreases, thus displaying a destabilizing effect. The observed destabilizing effect is stronger with decreasing n. A physical interpretation may be related to the reduction of

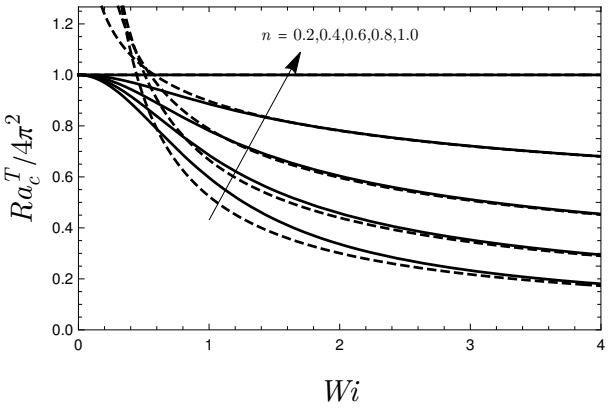

FIG. 5. Critical Rayleigh number for pseudoplastic fluids, normalized by the critical one for Newtonian fluids ($4\pi^2$), versus the Darcy-Weissenberg number. Results obtained for transverse rolls with $a = 2$ and different values of n. The dashed lines in this figure are relative to the power-law model.

viscosity with increasing shear-thinning effects, making the fluid less resistant to thermal buoyancy forces. Dashed curves in Fig. 5 represent the results obtained by (51a), which coincide with results present in the literature when power–law model is considered. Moreover, as can be seen in this figure, dashed curves coincide with continuous ones if the Darcy-Weissenberg number exceeds a special value Wi_t which depends on n. Without loss of generality, one can approximate this value by $Wi_t \approx 1$. We also remark that, for $Wi < Wi_t$, dashed curves tend to infinity, indicating that the power–law model becomes singular for weakly non-Newtonian fluids in agreement with what is found in[4]. Consequently, we can conclude that the power–law model and the Darcy-Carreau model lead to similar results in the strongly non-Newtonian regime (i.e. $Wi > Wi_t \approx 1$) while a significant qualitative difference between the two models is observed in the weakly non-Newtonian regime (i.e. $Wi < Wi_t$).
Figure 6 shows that the critical wavenumber for pseudoplastic fluids is less than $k_c = \pi$, namely the value associated to Newtonian fluids. This implies that emerging transverse convection rolls have a larger cross-section for pseudoplastic fluids than for Newtonian fluids.

Figure 7 shows the results for the dilatant ($n > 1$), as well as for the Newtonian fluids ($n = 1$). The critical Rayleigh number is again normalized by $4\pi^2$. We can observe that in this case the effect of increasing Wi generates a stabilizing effect. Such a result is also expected, since for dilatant fluids the viscosity increases with Wi, generating more resistance to the destabilizing thermal buoyancy forces. Dashed curves represent the results obtained by (51c), which are nearly similar with those of the power-law model provided that $Wi > Wi_t \approx 1$. On the other hand, for $Wi < Wi_t$, the critical Rayleigh number predicted by the Carreau model (51c) tends to $4\pi^2$, while it goes to zero with the power-law model, as predicted by[4]. Finally, we recall that, for the dilatant fluids, the critical wave number for longitudinal rolls is a constant (eq. (50b)).

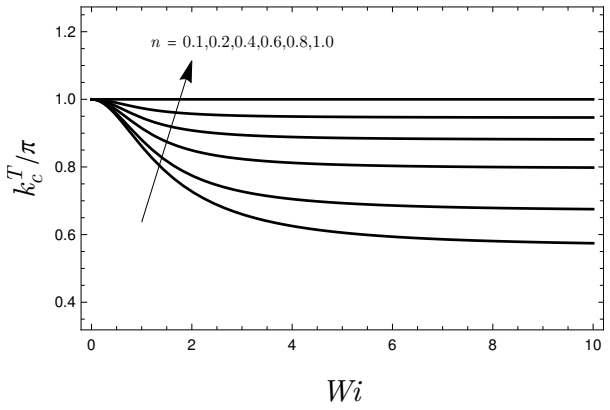

FIG. 6. Critical wave number for pseudoplastic fluids versus the Darcy-Weissenberg number. Results obtained for transverse rolls with $a = 2$ and different values of n.

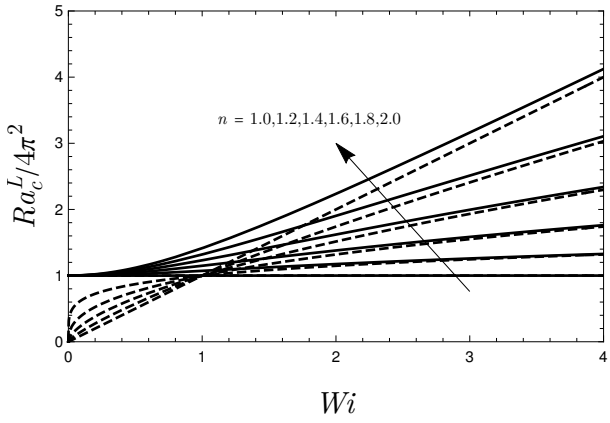

FIG. 7. Critical Rayleigh number for dilatant fluids, normalized by the critical one for Newtonian fluids ($4\pi^2$), versus the Darcy-Weissenberg number. Results obtained for longitudinal rolls with $a = 2$ and different values of n. The dashed lines in this figure are relative to the power-law model.

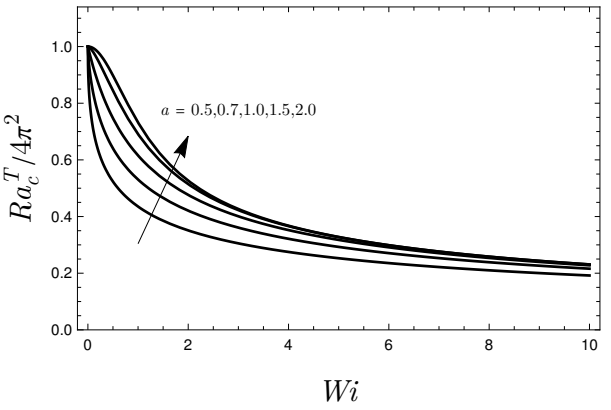

FIG. 8. Critical Rayleigh number for pseudoplastic fluids, normalized by the critical one for Newtonian fluids ($4\pi^2$), versus the Darcy-Weissenberg number. Results obtained for transverse rolls with $n = 0.5$ and different values of a.

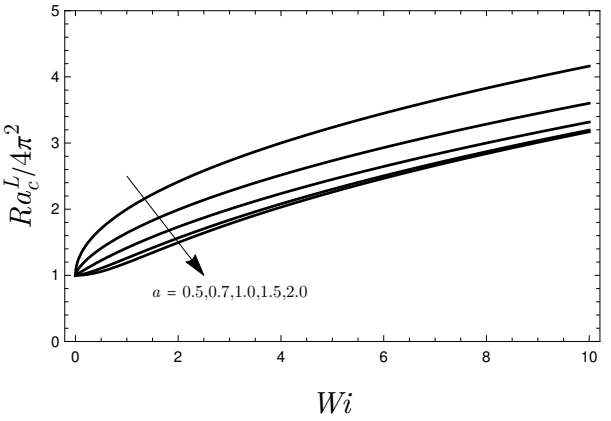

FIG. 9. Critical Rayleigh number for dilatant fluids, normalized by the critical one for Newtonian fluids ($4\pi^2$), versus the Darcy-Weissenberg number. Results obtained for longitudinal rolls with $n = 1.5$ and different values of a.

The effect of the Yasuda parameter a on the critical Rayleigh number for both pseudoplastic and dilatant fluids is illustrated in Figures 8 and 9, respectively, for a fixed value of n. These two figures show that, as a decreases, the critical Rayleigh number for pseudoplastic fluids decreases while it increases for dilatant fluids. The parameter a has then a stabilizing effect for pseudoplastic fluids and a destabilizing effect for dilatant fluids. We also note that, for a high value of Wi, the critical Rayleigh number becomes less dependent on a meaning that, in this limit, there is no significant difference between the Darcy-Carreau-Yasuda model and the Darcy-Carreau model.

III. ENERGY BUDGET ANALYSIS

An energy budget analysis is proposed in order to gather further insights into the physical mechanisms underlying the instability of shear thinning and shear thickening fluids. The starting point is the momentum equation (37) written for the most unstable modes, namely transverse rolls for $n < 1$ and longitudinal rolls for $n > 1$. For the sake of conciseness, the procedure is illustrated here only for transverse rolls with $n < 1$,

$$(1+Wi^a)^{\frac{n-1}{a}}\left[1+\frac{(n-1)\,Wi^a}{1+Wi^a}\right]u=-\frac{\partial p}{\partial x} \qquad (56)$$

$$(1+Wi^a)^{\frac{n-1}{a}}\,w=-\frac{\partial p}{\partial z}+Ra\,\theta \qquad (57)$$

On multiplying by the complex conjugate of u and w equations (56) and (57), respectively, and by adding the two resulting equations, we obtain

$$(1+Wi^a)^{\frac{n-1}{a}}\left[|u|^2+|w|^2+\frac{(n-1)\,Wi^a}{1+Wi^a}\,|u|^2\right]=$$

$$-\overline{u}\frac{\partial p}{\partial x}-\overline{w}\frac{\partial p}{\partial z}+Ra\,\overline{w}\,\theta \tag{58}$$

where the overline stands for the complex conjugate.

We integrate equation (58) over the range $0\leq z\leq 1$. By employing both the normal mode formulation (i.e. $\partial p/\partial x = ikp$) and the local mass balance equation (i.e. $-ik\overline{u} = -\partial\overline{w}/\partial z$) , the terms $-\overline{u}\,\partial p/\partial x-\overline{w}\,\partial p/\partial z$ may be written as $-\partial(p\overline{w})/\partial z$. As the the horizontal boundaries are impermeable, the integral of $-\partial(p\overline{w})/\partial z$ over the range $0\leq z\leq 1$ is zero. Thus, we obtain a relationship for the fluctuating energy at the neutral stability condition

$$\mathrm{e_{th}}+\mathrm{e_{nN}}+\mathrm{e_d}=0 \tag{59}$$

where the different contributions are given by

$$\mathrm{e_{th}} = Ra_c\int_0^1(\overline{w}\,\theta)\,\mathrm{d}z$$

$$\mathrm{e_{nN}} = (1+Wi^a)^{\frac{n-1}{a}}\,\frac{(1-n)Wi^a}{1+Wi^a}\int_0^1|u|^2\,\mathrm{d}z$$

$$\mathrm{e_d} = -(1+Wi^a)^{\frac{n-1}{a}}\int_0^1(|u|^2+|w|^2)\,\mathrm{d}z \tag{60}$$

The energy $\mathrm{e_{th}}$ corresponds to the part of the thermal buoyancy contribution due to the imposed temperature gradient, $\mathrm{e_{nN}}$ represents a non-Newtonian hydrodynamic energy production generated by the interaction of the basic flow with the horizontal perturbation velocity u and $\mathrm{e_d}$ is the viscous dissipation energy.

We notice that $\mathrm{e_d}$ is negative, indicating that the dissipation contribution produces a stabilization effect. Similarly to $\mathrm{e_{th}}$, the contribution $\mathrm{e_{nN}}$ is positive for shear thinning fluids ($n<1$) indicating the destabilizing effect of the non-Newtonian nature of the fluid. This destabilizing effect is due to the coupling between the throughflow and the non-Newtonian nature of the fluid.

By normalizing the above contributions with the absolute value $|\mathrm{e_d}|$, the momentum energy budget then becomes,

$$\mathrm{E_{th}}+\mathrm{E_{nN}} = 1 \tag{61}$$

with $\mathrm{E_{th}} = \frac{\mathrm{e_{th}}}{|\mathrm{e_d}|}$ and $\mathrm{E_{nN}} = \frac{\mathrm{e_{nN}}}{|\mathrm{e_d}|}$.
The expressions of the perturbations u, w and θ may be obtained analytically by using Eqs. (39), (41) and the continuity equation. They read,

$$\theta = \tilde{\theta}\exp(ik_c^T x - ik_c^T Pet)\sin(\pi z) \tag{62}$$

$$w = ((k_c^T)^2+\pi^2)\,\tilde{\theta}\exp(ik_c^T x - ik_c^T Pet)\sin(\pi z) \tag{63}$$

$$u = \frac{i\pi}{k_c^T}((k_c^T)^2+\pi^2)\,\tilde{\theta}\exp(ik_c^T x - ik_c^T Pet)\cos(\pi z) \tag{64}$$

By taking into account the above equations with the expression of the critical Rayleigh number for transverse rolls defined by (49a), yields simple analytical expressions of $\mathrm{E_{th}}$ and $\mathrm{E_{nN}}$,

$$\mathrm{E_{th}} = \frac{(k_c^T)^2\pi^2}{((k_c^T)^2+\pi^2)^2}\left[1+\left(\frac{1+nWi^a}{1+Wi^a}\right)^{\frac{1}{2}}\right]^2$$

$$\mathrm{E_{nN}} = \frac{\pi^2(1-n)Wi^a}{(1+Wi^a)((k_c^T)^2+\pi^2)} \tag{65}$$

The two contributions $\mathrm{E_{nN}}$ and $\mathrm{E_{th}}$ in the strongly non-Newtonian regime (i.e. large Wi) and in the weakly non-Newtonian regime (i.e. small Wi) may be written as,

$$\mathrm{E_{th}} = \sqrt{n}$$

$$\mathrm{E_{nN}} = 1-\sqrt{n}$$

for $Wi\gg 1$, and

$$\mathrm{E_{th}} = 1-\frac{1}{2}(1-n)Wi^a$$

$$\mathrm{E_{nN}} = \frac{1}{2}(1-n)Wi^a$$

for $Wi\ll 1$.
In these two limits, we remark that the non–Newtonian hydrodynamic energy $\mathrm{E_{nN}}$ increases when the index n decreases from $n=1$ to $n=0$, while the opposite occurs for $\mathrm{E_{th}}$. The reason is that for decreasing n, the shear-thinning nature of the non-Newtonian fluid becomes predominant.

Figures 10 and 11 show the thermal and non–Newtonian energy variation with Wi for $a=0.5$ and $a=2$ respectively. Three cases of n are considered. We can observe that the non–Newtonian energy $\mathrm{E_{nN}}$ increases as Wi increases, meaning that more energy is yielded by the basic throughflow to disturbances. As a consequence, $\mathrm{E_{th}}$ decreases, indicating that less thermal energy is needed to trigger the instability. For high values of Wi, the two energies tend asymptotically to constant values. The asymptotic value of $\mathrm{E_{nN}}$ may be explained physically by invoking the characteristic time of the fluid λ^* and the characteristic time of the flow which is the inverse of the porous shear rate $\dot{\gamma}_p^*$. The Darcy-Weissenberg number is the ratio between these two characteristic times. As the linear dynamics occurs at the smaller time, this dynamics is ruled by the characteristic time of the flow for large Wi. Therefore, at this time scale, no interaction may be expected between the non-Newtonian characteristics of the fluid and the basic throughflow, leading to a constant energy $\mathrm{E_{nN}}$.

We also observe in figures 10 and 11 that for small values of n the curves of thermal and non–Newtonian energies intersect. When this occurs, it means that there is a swap on the dominant disturbance energy. In order to evaluate the exact value of Wi number for which the curves intersect for each a and n, one may solve the equation $\mathrm{E_{th}}=\mathrm{E_{nN}}$, yielding to

$$Wi^a = \frac{3}{1-4n} \tag{66}$$

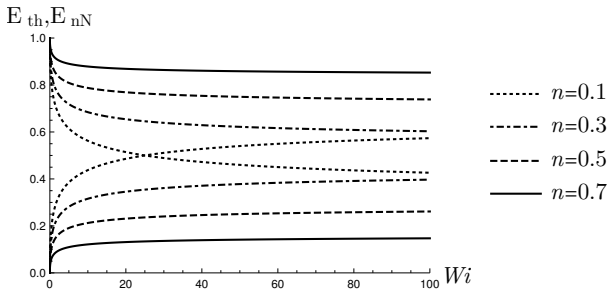

FIG. 10. Energy budget analysis for the case $a = 0.5$. Upper curves represent the thermal energy (E_{th}) and lower ones the non–Newtonian energy (E_{nN}).

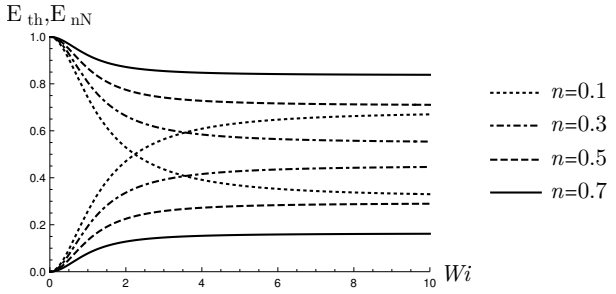

FIG. 11. Energy budget analysis for the case $a = 2$. Upper curves represent the thermal energy (E_{th}) and lower ones the non–Newtonian energy (E_{nN}).

considering that Wi^a may assume just positive values, the curves will intersect just when $n < 1/4$, or even for $n = 1/4$ if $Wi \to \infty$.

For dilatant fluids ($n > 1$), longitudinal rolls are the dominant mode of instability with $u = 0$. In that case, the fluctuating energies are reduced to e_d and e_{th} while the non-Newtonian contribution e_{nN} vanishes. For longitudinal rolls, e_d is defined as,

$$e_d = -(1+Wi^a)^{\frac{n-1}{a}} \int_0^1 (|u|^2 + |w|^2)\,dz$$

In that case, the momentum energy balance is

$$e_{th} + e_d = 0. \tag{67}$$

Equation (67) states that the dissipation energy must be balanced by the thermal buoyancy energy without the contribution of e_{nN}. As e_d decreases with Wi, then e_{th} will observe an increase with Wi, attesting the stabilizing effect for dilatant fluids as it is predicted by the previous normal mode analysis.

IV. DISCUSSION OF THE RESULTS IN RELATION TO COMMON POROUS MEDIA AND TO EXPERIMENTS IN HELE-SHAW CELL

A. Application to common porous media

This section aims to analyse the interplay between the non–Newtonian nature of the fluid and the intrinsic porous media characteristics at the onset of mixed convection. We have shown that the thermal instability threshold Ra_c depends on the three dimensionless parameters n, a and Wi. The latter can be written as

$$Wi = \lambda^* f_p^{\frac{1}{n-1}} (\Phi K)^{-\frac{1}{2}} U_0^*, \tag{68}$$

with

$$f_p = 8^{-\frac{n+1}{2}} 2 \left(\frac{3n+1}{n}\right)^n. \tag{69}$$

If we introduce the dimensionless time characteristic of the fluid $\lambda = \frac{\lambda^*}{H^2/\kappa}$, the Darcy number $Da = \frac{K}{H^2}$ and the Péclet number Pe, equation (68) may be written as,

$$Wi = \lambda\, \dot{\gamma}_p, \tag{70}$$

where $\dot{\gamma}_p$ is the dimensionless porous shear–rate and is defined as

$$\dot{\gamma}_p = f_p^{\frac{1}{n-1}} (\Phi Da)^{-\frac{1}{2}} Pe. \tag{71}$$

For shear-thinning fluids, the characteristic time of the fluid, λ^*, may vary from 0.1 s to 100 s. For common porous materials the values of the permeability K vary widely from $10^{-20}\,m^2$ to $10^{-7}\,m^2$ (see for instance Nield and Bejan[2]), a typical value of the porosity ϕ is 0.35, while the filtration velocity U_0^* may hardly be higher than $4\times10^{-4}\,m\,s^{-1}$. If we fix $H = 4\times10^{-2}\,m$ and $\kappa = 10^{-7}\,m^2\,s^{-1}$, then the dimensionless characteristic time of the fluid λ may vary approximately from 10^{-5} to 10^{-2}, while the product of Darcy number Da and the porosity Φ may vary from 10^{-5} to 10^{-18}. The impact of the porous properties on the onset of convection may be examined by fixing λ, n and Pe and by varying the product (ΦDa). While the effect of the throughflow may be identified by fixing λ, n and (ΦDa) with a variable Pe. Figure 12 shows the dependence on (ΦDa) of Ra_c^T associated with pseudoplastic fluids for a prescribed value of Péclet number $Pe = 4$ corrresponding to $U_0^* = 4\times10^{-5}\,m\,s^{-1}$. We can observe that the effect of the term ϕDa is to increase the critical Rayleigh number. Physically, it means than a more permeable porous material may delay the onset of mixed convection. On the contrary, for a fixed value of (ΦDa), the critical Rayleigh number decreases as n decreases, attesting that the shear-thinning charater of the fluid enhances the onset of convection. On the other hand, the effect of Pe on Ra_c^T may be seen in Figure 13 for $(\Phi Da) = 10^{-5}$. The effect of varying Pe for a fixed (ΦDa) is qualitatively the same as varying Wi. For both figures, data used for n and λ^* were extracted from Darbouli et al.[20]. These authors conducted experiments in a

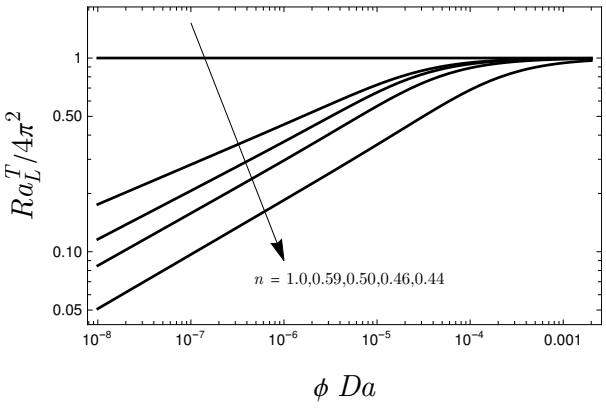

FIG. 12. Critical Rayleigh number for pseudoplastic fluids as a function of ϕDa. Results obtained for transverse rolls with $a = 2$ and different values of n.

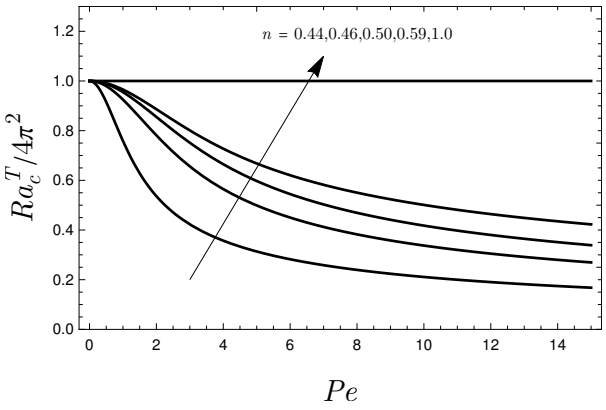

FIG. 13. Critical Rayleigh number for pseudoplastic fluids as a function of Pe. Results obtained for transverse rolls with $a = 2$ and different values of n.

Rayleigh–Bénard configuration without a solid matrix, in order to investigate the onset of convection in shear–thinning fluids.

As already discussed before, two regimes of instability can be identified from the critical conditions at the onset of mixed convection. A strongly non–Newtonian regime and a weakly non–Newtonian one exist depending on the Darcy-Weissenberg number. The first is the one in which the power–law model and the Carreau model results almost coincide, while the second is the one in which these models disagree significantly. As an approximate value of the Darcy-Weissenberg number, and without any loss of generality, we here set $Wi \sim 1$ as a special value where a transition occurs between the two regimes. From equation (70) it is possible to know, for each value of $\dot{\gamma}_p$, the value of λ in which this transition should occurs, and it is given by equation

$$\lambda = \frac{1}{\dot{\gamma}_p}. \tag{72}$$

Figure 14 shows the characteristic time of the fluid as a function of the porous shear–rate with the transition curve between weakly and strongly non–Newtonian regimes.

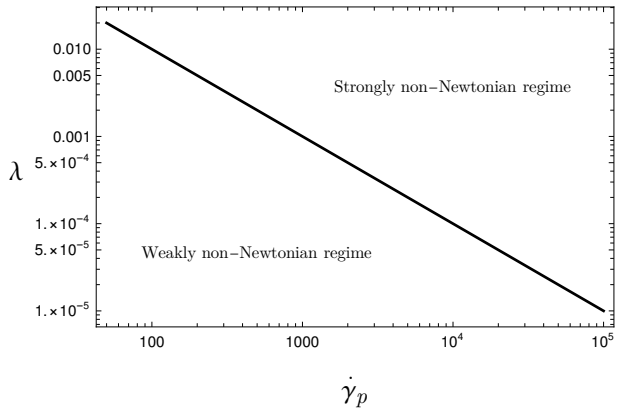

FIG. 14. Transition map between the weakly and the strongly non-Newtonian regimes of instability.

B. Comparison with experiments in Hele-Shaw cell

In this section some experimental data for the onset of convection present in literature are compared with the present theoretical results based on Darcy-Carreau and Darcy-Carreau-Yasuda rheological models. Recently, Petrolo et al.[15] investigated theoretically and experimentally the onset of convection under a horizontal throughflow of pseudoplastic fluids in a Hele–Shaw cell. In order to make possible such a comparison, it is necessary to reformulate the results in terms of the Rayleigh number used in Petrolo et al.[15], denoted here as Ra^* and defined by

$$Ra^* = \frac{\rho_0 \beta\, g\, K^*\, H^n\, \Delta T^*}{\eta\, \kappa_m^n}, \tag{73}$$

where $K^* = (\frac{b}{2})^{n+1}(\frac{n}{2n+1})^n$ is the permeability used in experiments to evaluate the Rayleigh number, b being the small width of the Hele–Shaw cell.
The relation between Ra^* and our Ra, evaluated by equation (49a) may be written as,

$$Ra^* = \Phi Ra \tag{74}$$

with

$$\Phi = 12 \left(\frac{H}{\kappa}\right)^{n-1} \frac{\mu_0}{\eta} \frac{b^{n-1}}{2^{n+1}} \left(\frac{n}{2n+1}\right)^n \tag{75}$$

Except for μ_0, all data needed to evaluate Φ and Darcy-Weissenberg number Wi are reported in Table 1 in Petrolo et al.[15]. The data related to μ_0 are not documented in Petrolo et al.[15]. Nevertheless, in supplementary material of Petrolo et al.[15], the variations of the apparent viscosity μ_a as a function of the average shear rate are represented for both experiments 4 and 7. Estimation of μ_0 is then possible by fitting the expression of μ_a given in the present study by Darcy-Carreau

TABLE I. Estimated coefficients of the Carreau–Yasuda model using data for experiment 4 in Petrolo et al.[15].

	Exp.	Estimate	Standard Error
μ_0	4	0.135022	0.001362
a	4	0.586851	0.00920399
μ_0	7	0.583125	0.050362
a	7	2.89781	0.83957

and Darcy-Carreau-Yasuda rheological models with the results associated to experiments 4 and 7. A similar approach is not possible for some other experiments conducted in Petrolo et al.[15], due to lack of information on the behavior of the apparent viscosity μ_a as a function of the average shear rate.

Having in mind the expression (9) of the apparent viscosity given by the Carreau–Yasuda model, where λ^* and $\dot{\gamma}_p$ are given by (8) and (4), respectively, and where

$$\frac{\eta_{ef}}{\eta} = f_{hs} K^{\frac{1-n}{2}} \tag{76}$$

with $f_{hs} = 3^{(-\frac{n+1}{2})}(\frac{2n+1}{n})^n$, $K = \frac{b^2}{12}$, one may recover μ_0 and the Yasuda parameter a based on the experimental data of the evolution of the apparent viscosity with the average shear-rate.

For the experiment 4 the fluid properties are given in Petrolo et al.[15] and read $n = 0.66$ and $\eta = 0.07$. Considering the experimental data given by the authors on the suplementary material the parameters μ_0 and a are estimated. Figure 1 in section I shows the experimental data (dots) and the Carreau–Yasuda model fit (continuous line) for the best-fitted a.

Table I show the parameters recovered from the experimental data. We note that the properties of the fluids used in experiments 4 and 6 in Petrolo et al.[15] are similar. Therefore, the estimated value of μ_0 is also taken to be the same for both experiments 4 and 6.

For experiments 7 and 2, the fluid characteristics are $n = 0.55$ and $\eta = 0.1$. Figure 15 shows the theoretical fit of the Carreau–Yasuda model over the experimental data. Table I shows the result for μ_0. In this case, we observed that variations of a have no significant effects on the results. For this reason the parameter a was fixed to $a = 2$ without any loss of generality.

In table II, we report the discrepancy between the measured values of critical Rayleigh number $Ra_c^{*,E}$ for the experiments analysed here and the theoretical values $Ra_c^{*,T}$. The values of Wi here were calculated based on the definition (21) by using the experimental data.

A rapid inspection of Table II shows that the discrepancy between theory and experiments 2 and 7 is relatively large. We note that their respective values of Darcy-Weissenberg number are also large, meaning that we are dealing with a strongly non-Newtonian regime. In this regime, as reported in Table II, we found that the theoretical value of the critical Rayleigh number $Ra_c^{*,pl}$ associated to power-law model is almost equal to $Ra_c^{*,T}$. Therefore, we concluded that temporal linear stability predictions stemming from both rheological

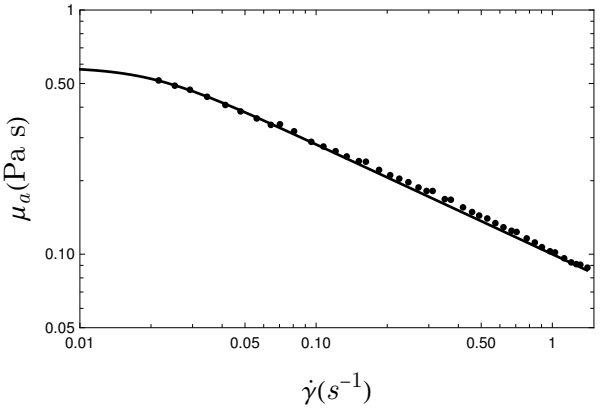

FIG. 15. Data from experiment 7 of[15] and fitted model, for $a = 2$.

TABLE II. Critical Rayleigh number $Ra_c^{*,E}$, index n and Pe as determined experimentally in[15] and the corresponding Darcy-Weissenberg number Wi estimated by considering experimental data. $Ra_c^{*,T}$ and $Ra_c^{*,pl}$ are respectively the critical Rayleigh number determined in the present work and the one obtained by using power law model[4].

Exp.	n	Pe	Wi	$Ra_c^{*,T}$	$\frac{Ra_c^{*,T}-Ra_c^{*,E}}{Ra_c^{*,E}}$	$Ra_c^{*,pl}$	$\frac{Ra_c^{*,pl}-Ra_c^{*,E}}{Ra_c^{*,E}}$
2	0.55	52	14.96	5.06	-18%	5.05	-19%
4	0.66	52	2.03	8.52	2.6%	8.46	1.9%
6	0.66	34	0.88	7.14	13%	9.77	55%
7	0.55	34	6.52	6.13	30%	6.12	30%

models, namely Darcy-Carreau-Yasuda and power-law models present the same discrepancy with experiments for relatively high values of Darcy-Weissenberg number. On the other hand, Table II shows that the observed discrepency between theory and experiments is significantly reduced for experiments 4 and 6 with the respective Darcy-Weissenberg number $Wi = 2.03$ and $Wi = 0.88$ respectively. As reported in Table II for both experiments, theory overestimates the critical Rayleigh number by 2.6% and 13%. In contrast to Darcy-Carreau-Yasuda model, we noticed that the power law model predictions lead to a large discrepancy between theory and experiments for $Wi = 0.88$.

Table III shows a good agreement between the critical wavenumber determined experimentally and the critical wavenumber predicted by temporal linear stability analysis.

Before the end of this section, a discussion is made on the comparison between experimental results and the predictions of the present temporal linear stability analysis. We raise some questions that may lead to interesting future paths of investigation. They are:

- The reasonable theoretical overestimation of the critical Rayleigh number compared with experiments 4 and 6 may be attributed to the the subcritical bifurcation nature at the onset of mixed convection. It is then necessary to investigate the contribution of the nonlinearities by conducting at least a weakly nonlinear stability approach.

TABLE III. Critical wave number from experimental results (k_c^E) and theory (k_c^T).

Exp.	k_c^T	$\frac{k_c^T - k_c^E}{k_c^E}$
2	2.71	−9.4%
4	2.71	−5.2%
6	2.97	−2.6%
7	3.01	8.3%

• As we are dealing with an open flow configuration, the absolute and convective nature of the instability must be taken into account (see the recent book by Barletta[21]). The convective or absolute nature of the instability was studied by Delache et al.[22] in convection under an imposed throughflow in porous media for Newtonian fluids. In relation to experiments, the most interesting result stemming from Delache et al.[22] is that the border between the convective and the absolute instability of moving transverse rolls corresponds perfectly to the experimentally observed transition from transverse rolls to longitudinal rolls and vice versa. At the threshold of absolute instability, the emerging transverse rolls are found to oscillate with a selected unique frequency. Moreover, by using a weakly nonlinear approach, Delache and Ouarzazi[23] showed that in the convectively unstable region, permanent disturbances may trigger the instability with a broad band of frequencies that may be amplified. Therefore, and from experimental point of view, the distinction between convective and absolute instability may be realized by inspecting the frequency spectrum at the onset of the instability: a peak of frequency is a signature of absolute instability while a broad frequency spectrum is associated to convective instabilities. Unfortunately, we emphasize that there is no information available in Petrolo et al.[15] about the frequency spectrum of the observed moving transverse rolls. Such information is necessary to discriminate between the self-dynamic of mixed convection patterns in the absolute instability regime and the transverse rolls actually observed in experiments that may arise from spatial amplification of some persistent perturbations of the flow in the convectively unstable regime. Therefore and in order to well understand the experimental results, a spatio-temporal stability approach is needed and compared with more experimental data that include the frequency spectrum.

• Finally, we emphasize that the theoretical model developed here does not take into account the influence of the yield stress effects observed in Petrolo et al.[15] .

V. CONCLUSION

The motivation of the present paper arose from the study by Barletta and Nield[4] on the linear stability problem of a non-Newtonian inelastic fluid in porous media subject simultaneously to a negative vertical temperature gradient and to a horizontal throughflow and also from recent experiments conducted by Petrolo et al.[15] for shear-thinning fluids in a Hele-Shaw cell. In Barletta and Nield[4], the non-Newtonian fluid is assumed to be of power–law type. The present paper improved their work by introducing a new rheological model, namely a Darcy–Carreau–Yasuda model which extends to porous media the well known Carreau–Yasuda model, usually employed in a non-Newtonian fluid clear of solid material. Unlike the power–law model, the Darcy–Carreau–Yasuda model has the advantage to describe in a regular manner the behaviour of the fluid viscosity at low shear rate to high shear rate regions. Five dimensionless parameters are introduced: The Darcy–Rayleigh number Ra, the Péclet number Pe, the Darcy-Weissenberg number Wi, the Yasuda parameter a and the power-law exponent n. A temporal stability analysis indicates that the form of the most amplified instability depends on the nature of the fluid. For shear thinning fluids ($n < 1$), the oscillatory transverse rolls are favored above any other structures. While the most unstable disturbances are stationary longitudinal rolls for shear thickening fluid ($n > 1$).
By considering the limiting case of infinite Wi (i.e. strongly non-Newtonian regime), our rheological model is reduced asymptotically to the power–law case and the results are compared with those presented in Barletta and Nield[4]. It is then observed that comparison of the linear characteristics at the the onset of mixed-convection is in very good agreement. However, when considering the limit of small Wi (i.e. weakly non-Newtonian regime), a significant qualitative difference between the Darcy–Carreau–Yasuda and power–law models is observed. In this limit, the power law model predicts that pseudoplastic fluids are always linearly stable (i.e. $Ra_c \to \infty$), while dilatant fluids are always linearly unstable (i.e. $Ra_c = 0$). On the other hand, results stemming from the Darcy–Carreau–Yasuda model showed that the classical critical value $Ra_c = 4\pi^2$ associated with the Horton-Rodgers-Lapwood problem in recovered in the limit of zero Wi. In the weakly non-Newtonian regime ($Wi < 1$), it is observed a significant drop in critical Rayleigh number for pseudoplastic fluids as the Darcy-Weissenberg number Wi increases. This destabilizing effect becomes more effective as the non-Newtonian parameters n and a decrease. An energy analysis showed the existence of two energy contributions in addition to the dissipation energy. The first is the thermal buoyancy contribution due to the imposed temperature gradient and the second is the non-Newtonian hydrodynamic energy production due to the coupling between the throughflow, the non-Newtonian nature of the fluid and the x-component of the disturbed velocity. For small values of Wi, the dominant disturbance energy is the thermal buoyancy contribution, meanig that the instability has nearly the same characteristics as a Newtonian fluid. While for high values of Wi, the non-Newtonian hydrodynamic energy production dominates indicating that the instability is mainly due to shear-thinning effects. For moderate values of Wi, a competition is observed between the two instability mechanisms. In the case of shear thickenig fluids, the stabilizing effect of the Darcy-Weissenberg number may be explained physically as follows. Unlike the shear thinning fluids, there is no x-component of the disturbed velocity for longitudinal rolls. Consequently,

the non-Newtonian hydrodynamic energy production is zero and the thermal buoyancy contribution must balance the dissipation energy. As in shear-thickening fluids the viscosity increases with the magnitude of the imposed throughflow, it results an increase in the dissipation energy which induces an increase of the thermal buoyancy contribution. Therefore, more heating is needed to trigger the thermal instability.
The relevance of the theoretical results obtained in this paper is examined by giving realistic values of the imposed horizontal velocity, the characteristics of the porous medium and the rheological parameters to observe thermal instabilities of non-Newtonian inelastic fluids. Moreover, a discussion of the results is made in connection with experiments conducted by Petrolo et al.[15] for mixed convection of shear-thinning fluids in Hele-Shaw cell. Available data for some experiments in Petrolo et al.[15] and its supplementary material allowed to evaluate the critical Rayleigh number and wave number at the onset of mixed convection as predicted by the Darcy–Carreau–Yasuda and the power-law models. In this regard, a deep discussion about the comparison between theory and experiments is conducted in section IV B. We showed that, for both rhelogical models, the discrepancy between theory and experiments is relatively large for high values of the Darcy-Weissenberg number. On the other hand, the Darcy–Carreau–Yasuda model showed that the observed discrepency between theory and experiments is significantly reduced for small to moderate values of Darcy-Weissenberg number. In these conditions, we observed a reasonable theoretical overestimation of the critical Rayleigh number compared with experiments. Although these encouraging results which showed the relevance of the the Darcy–Carreau–Yasuda for moderate values of the Darcy-Weissenberg number, we believe that a weakly nonlinear study is necessary to evaluate the nonlinear effects on the supercritical/subcritical nature of the bifurcation in mixed convection of shear–thinning fluids. The weakly nonlinear stability analysis in the framework of Darcy–Carreau–Yasuda model is under consideration and will be the the subject of a future paper. We also mention that the net flow rate associated with the basic flow may yield a discrepancy between the convective instability threshold and the transition to absolute instability. Such a behaviour may add interesting new elements to the analysis of the comparison between the theory and the experiments. This task is also an opportunity for future developments of this research.

ACKNOWLEDGEMENTS

The author A. Barletta acknowledges the financial support from the grant PRIN 2017F7KZWS provided by the Italian Ministry of Education and Scientific Research. The author P. V. Brandão acknowledges the financial support from Coordenação de Aperfeiçoamento de Pessoal de Nível Superior - Brasil (CAPES) - Grant nº 88881. 174085/2018-01

DATA AVAILABILITY

The data that support the findings of this study are available on request from the corresponding author.

[1] B. Straughan, "Stability and Wave Motion in Porous Media," Springer, (2008).
[2] D. A. Nield, and A. Bejan, "Convection in Porous Media," 5th edition, Springer, (2017).
[3] A. Barletta, "Routes to Absolute Instability in Porous Media," New York: Springer, (2019).
[4] A. Barletta and D. A. Nield, "Linear instability of the horizontal throughflow in a plane porous layer saturated by a power–law fluid," Phys. Fluids 23, 013102 (2011)
[5] L. S. de B. Alves and A. Barletta, "Convective to absolute instability transition in the Prats flow of a power-law fluid," Int. J. Therm. Sci 94, 270 (2015)
[6] S. Hirata, LS de B. Alves, N. Delenda and M. N. Ouarzazi, "Convective and absolute instabilities in Rayleigh–Bénard–Poiseuille mixed convection for viscoelastic fluids," J. Fluid Mech. 765, 167 (2015).
[7] A. Taleb, H. BenHamed, M. N. Ouarzazi, and H. Beji, "Analytical and numerical analysis of bifurcations in thermal convection of viscoelastic fluids saturating a porous square box," Phys. Fluids 28(5), 053106 (2016).
[8] S. Hirata, LS. de B. Alves and M.N. Ouarzazi, "Linear onset of convective instability for Rayleigh-Bénard-Couette flows of viscoelastic fluids," J. Non-Newtonian Fluid Mech. 231, 79 (2016)
[9] M. Celli and A. Barletta, "Onset of convection in a non-Newtonian viscous flow through a horizontal porous channel," Int. J. Heat Mass Transfer 117, 1322 (2018)
[10] R. H. Christopher and S. Middleman, "Power-law flow through a packed tube," Ind. Eng. Chem. Fund. 4, no. 4, 422 (1965).
[11] D.A. Nield, "A Note on the Onset of Convection in a Layer of a Porous Medium Saturated by a Non–Newtonian Nanofluid of power–Law Type," Trans. Porous Media 87, 121 (2011).
[12] D.A. Nield, "A Further Note on the Onset of Convection in a Layer of a Porous Medium Saturated by a Non–Newtonian Fluid of power–Law Type," Trans. Porous Media 88, 187 (2011).
[13] P.V. Brandão and M.N. Ouarzazi, "Darcy–Carreau Model and Nonlinear Natural Convection for Pseudoplastic and Dilatant Fluids in Porous Media", Trans. Porous Media 136, 521 (2021).
[14] D.A.S. Rees, "Darcy–Bénard–Bingham convection," Phys. Fluids 32, 084107 (2020).
[15] D. Petrolo, L. Chiapponi, S. Longo, M. Celli, A. Barletta and V. Di Federico, "Onset of Darcy-Bénard convection under through flow of a shear thinning fluid," J. Fluid Mech. 889, R21 (2020).
[16] K. Yasuda, R. C. Armstrong and R. E. Cohen, "Shear flow properties of concentrated solutions of linear and star branched polystyrenes," Rheol. Acta 20, 163 (1981).
[17] M.H. Allouche, V. Botton, D. Henry, S. Millet, R. Usha and H. Ben Hadid, "Experimental determination of the viscosity at very low shear rate for shear thinning fluids by electrocapillarity," J. Non-Newtonian Fluid Mech. 215, 60 (2015)
[18] J.P. Pascal and H.Pascal, "Nonlinear effects on some unsteady non-Darcian flows through porous media," Int. J. Non-Linear Mech. 32(2), 361 (1997)
[19] S. Longo, V. Di Federico, L. Chiapponi and R. Archetti, "Experimental verification of power–law non–Newtonian axisymmetric porous gravity currents," J. Fluid Mech. 731, R2 (2013).
[20] M. Darbouli, C. Métivier, S. Leclerc, C. Nouar, M. Bouteera and D. Stemmelen, "Natural convection in shear-thinning fluids: Experimental investigations by MRI.," Int. J. Heat Mass Transfer 95, 742 (2016)
[21] A. Barletta, "Routes to Absolute Instability in Porous Media," Springer, New York, (2019).
[22] A. Delache, M.N. Ouarzazi and M. Combarnous, "Spatio-temporal stability analysis of mixed convection flows in porous media heated from below:comparison with experiments," Int. J. Heat Mass Transfer 50, 1485 (2007).
[23] A. Delache and M.N. Ouarzazi, "Weakly nonlinear interaction of mixed convection patterns in porous media heated from below," Int. J. Thermal Sci. 47, 709 (2008).

[24]M. Prats, "The effect of horizontal fluid flow on thermally induced convection currents in porous mediums," J. Geophys. Res. 71, 4835 (1966).